Unprecedented palladium(II) complex containing dipodal 1,3,4-thiadiazole derivative: Synthesis, structure, biological and thermal investigations

Leila Heidari,[a] Mitra Ghassemzadeh,*[a], Dieter Fenske,[b] Olaf Fuhr,[b] Maryam Saeidifar[c] and Farshid Mohsenzadeh[a]

[a] Department of Inorganic Chemistry, Chemistry & Chemical Engineering Research Center of Iran, Pajoohesh Blvd., 17th Km of Tehran–Karaj Highway, Tehran 14968-13151, Iran. Fax: +98 21 44787753; Tel: +98 21 44787706;
*Email: mghassemzadeh@ccerci.ac.ir (M. Ghassemzadeh)
[b] Institut für Nanotechnologie and Karlsruhe Nano Micro Facility (KNMF), Karlsruher Institut für Technologie, Hermann-von-Helmholtz-Platz 1, 76344 Eggenstein-Leopoldshafen, Germany
[c] Department of Nanotechnology and Advanced Materials, Materials and Energy Research Center, Karaj, Iran

Supporting Information

Synthesis and characterization of L

The *bis* thiadiazole, 1,4-*bis*(5-amino-1,3,4-thiadiazol-2-sulfanyl-methyl) benzene (**L**), can be prepared by the reaction of 2-amino-5-mercapto-1,3,4-thiadiazole with 4,4'-dibromoxylene in a molar ratio 2:1 in the presence of potassium hydroxide in ethanol (Scheme SS1). It was isolated as a white solid mass in excellent yield.

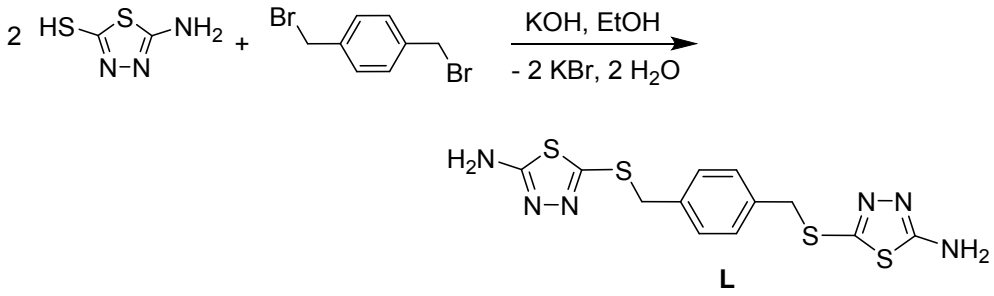

Scheme SS1 Synthesis route of **L**

The ligand, **L,** was prepared according to literature procedure.[1] A solution of *α,α′*-dibromo-*p*-xylene (1.5 g, 5.68 mmole) in ethanol (40 ml) was added dropwise to a solution of 2-amino-5-mercapto-1,3,4-thiadiazole (1.51 g, 11.36 mmole) in ethanol (30mL) containing potassium hydroxide (0.64 g, 11.36 mmole). The mixture was refluxed for 48 h. The residue was filtered off, washed twice with water and ethanol (2 x 10 mL of each solvent) and recrystallized from DMF. Yield: 1.88 g (90%), mp.: 260 °C (dec.). Elemental analysis: calcd. For $C_{12}H_{12}N_6S_4$ (368.52): C, 39.11; H, 3.28; N, 22.80 %. Found: C, 38.95; H, 3.24; N, 22.76 %. FT-IR (KBr, *v*, cm^{-1}): 3265 and 3106 (m, $v_{N–H}$), 2947(w), 2763(w), 1661(m), 1627(m, $v_{C=N}$), 1515(s), 1423(m, $v_{C=C\ Ar}$), 1385(w), 1322(w), 1239(w), 1064(s), 1043(m), 888(w), 834(w), 775(w), 683(w), 658(w,

$\nu_{C\text{-}S}$), 587(w), 504(w). LC/MS (API, in DMSO-CH_3CN): *m/z* = 369 $[M+1]^+$, 391 $[M + Na^+]$, 407 $[M + Na^+ + NH_4^+]$. ^1H NMR (δ, DMSO-d_6, 500 MHz): 4.29 (s, 4H, CH_2S), 7.30-7.31 (d, 4H, CH Ar), 7.33 (s, 4H, NH_2).

The ^1H NMR spectrum of **L** in DMSO includes three signals at δ = 4.29, 7.31, and 7.33 ppm assignable to the S–CH_2 protons, aromatic ring protons, and NH_2 groups, respectively. The pattern of the ^1H NMR spectra of **L** indicates that the dipodal compound possesses an inversion center; therefore, its structure can be described as a centrosymmetric one (Fig. FS1). The LC/MS spectrum of **L** shows a peak at *m/z* = 369 $[M+1]^+$, which confirms the formation of **L** (Fig. SF2)**.** FT-IR spectra of **L** show two bands at 3265 cm^{-1} and 3253, which can be assigned to valence vibrations of NH_2 groups. Furthermore, the C=N and C–S vibration bands of **L** can be observed at 1627 and 725 cm^{-1}, respectively (Fig. SF3).

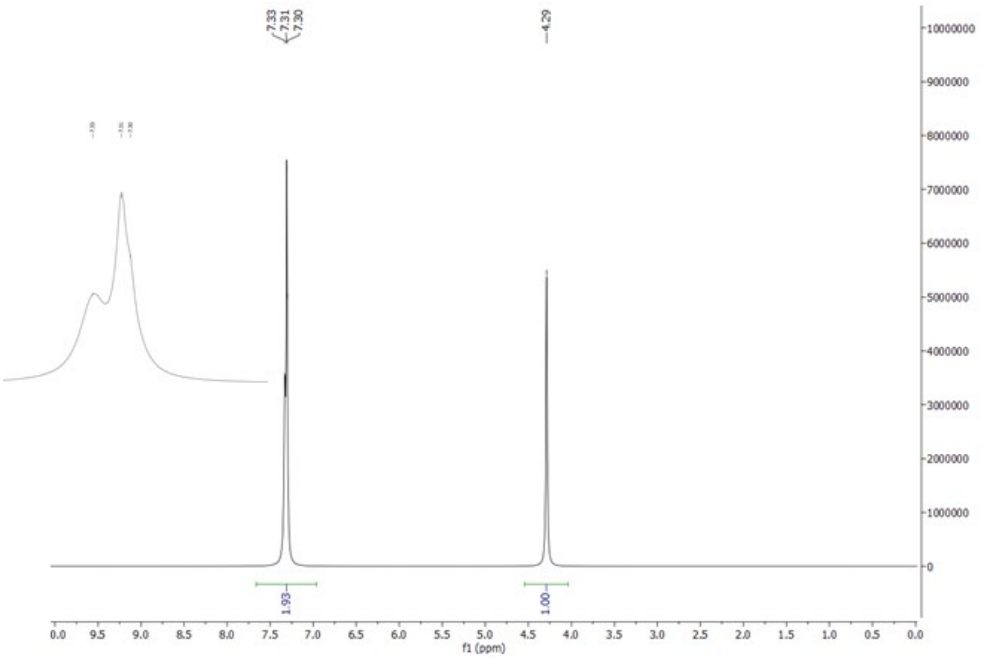

Fig. SF1 ^{1}H NMR spectrum of **L** in DMSO-d_6 at 25 °C (the peaks of DMSO are omitted).

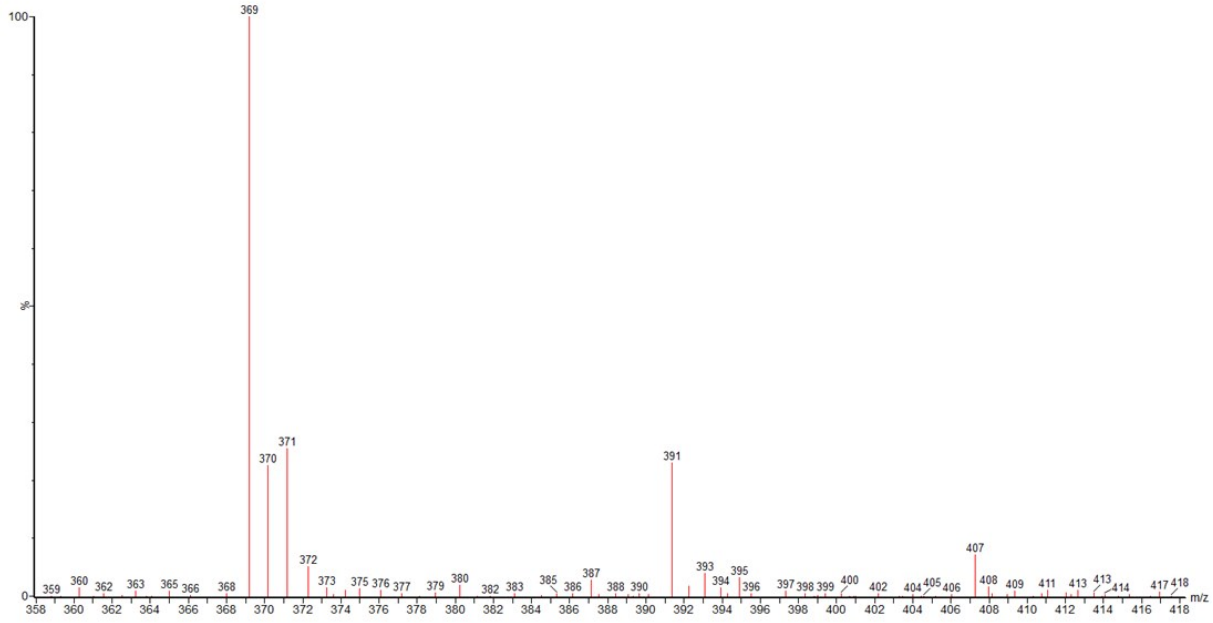

Fig. SF2 LC/MS spectrum of **L**.

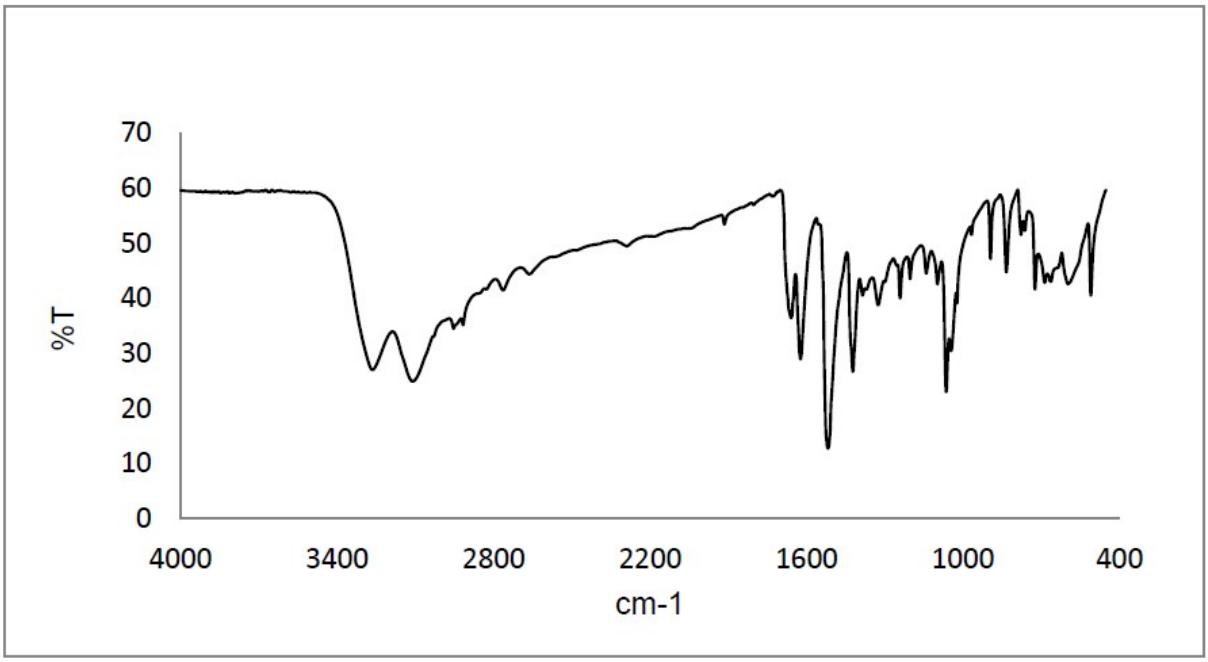

Fig. SF3 FT-IR spectrum of **L**.

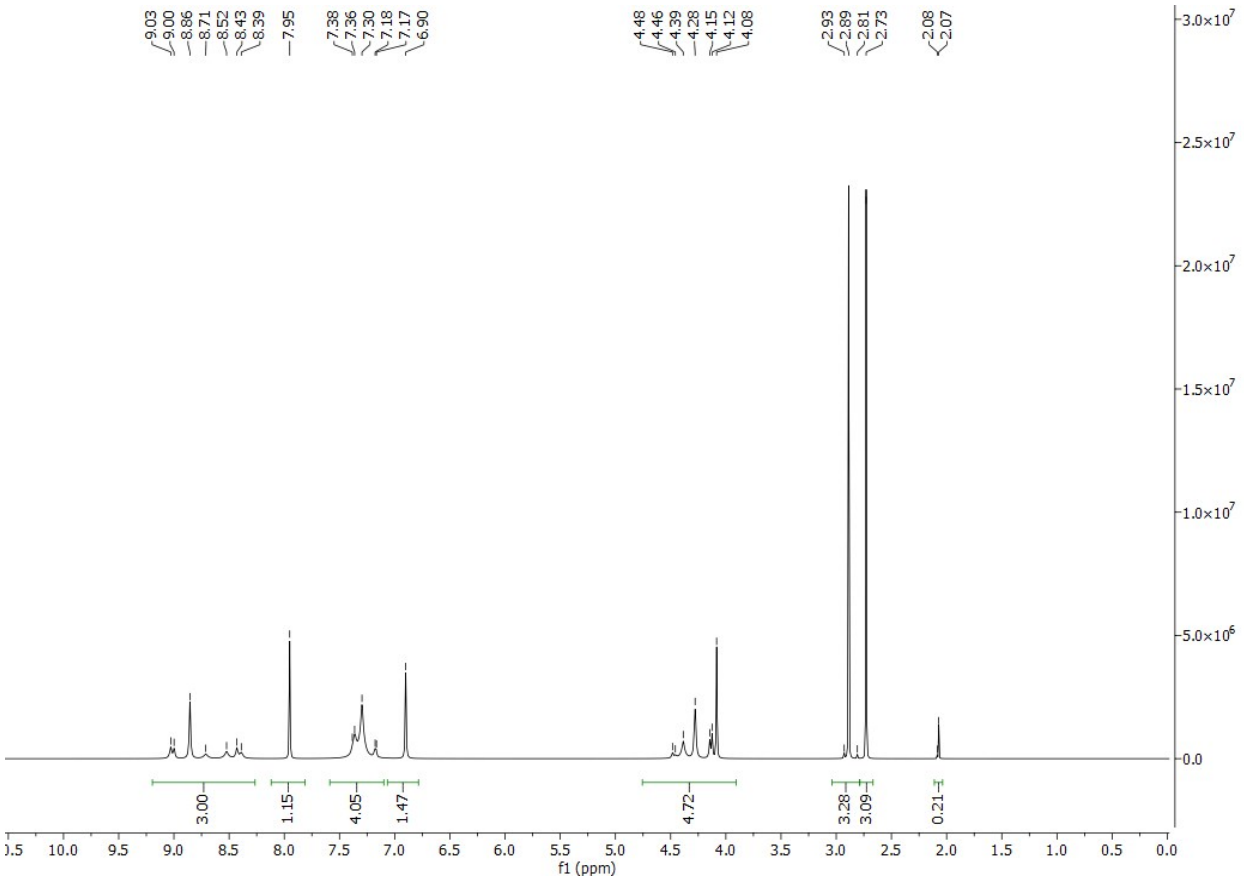

Fig. SF4 ^{1}H NMR spectrum of **1**·DMF in DMSO-d_6 at 25 °C (the peaks of DMSO are omitted).

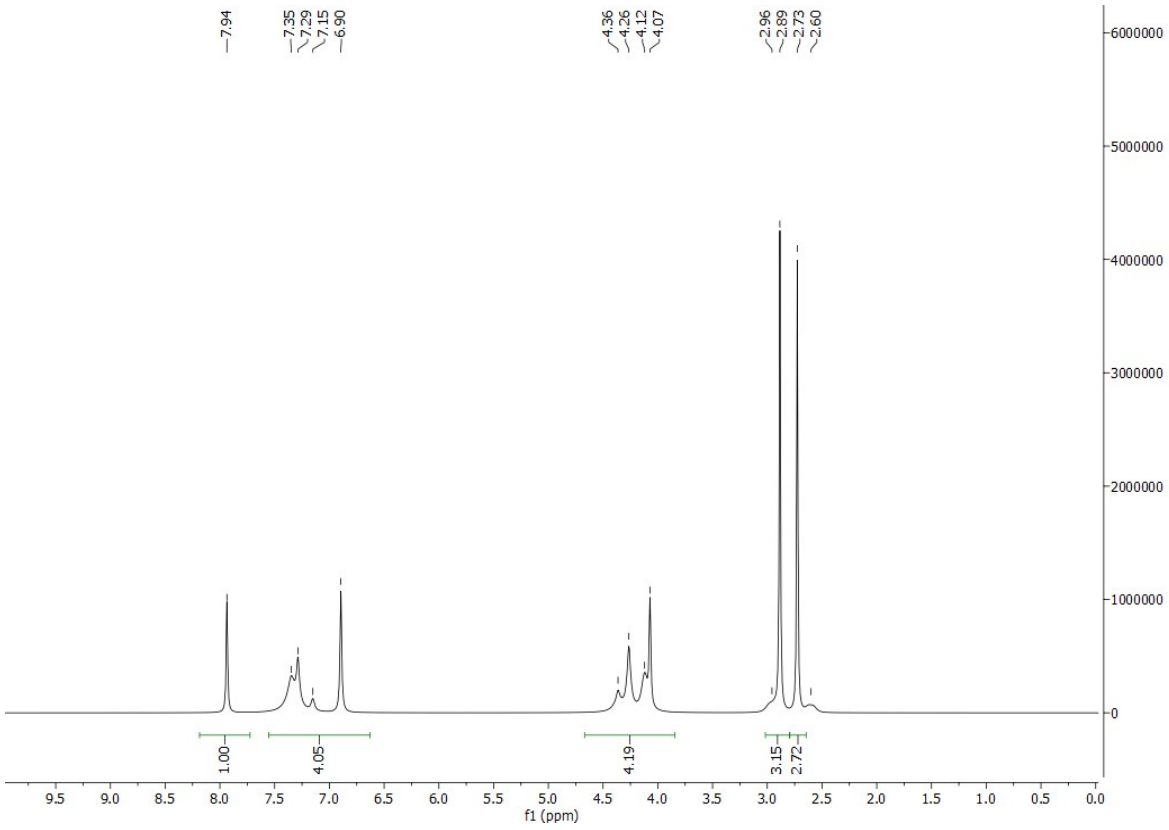

Fig. SF5 ^{1}H NMR spectrum of **1**·DMF in DMSO-d_6 + D_2O at 25 °C (the peaks of DMSO and D_2O are omitted).

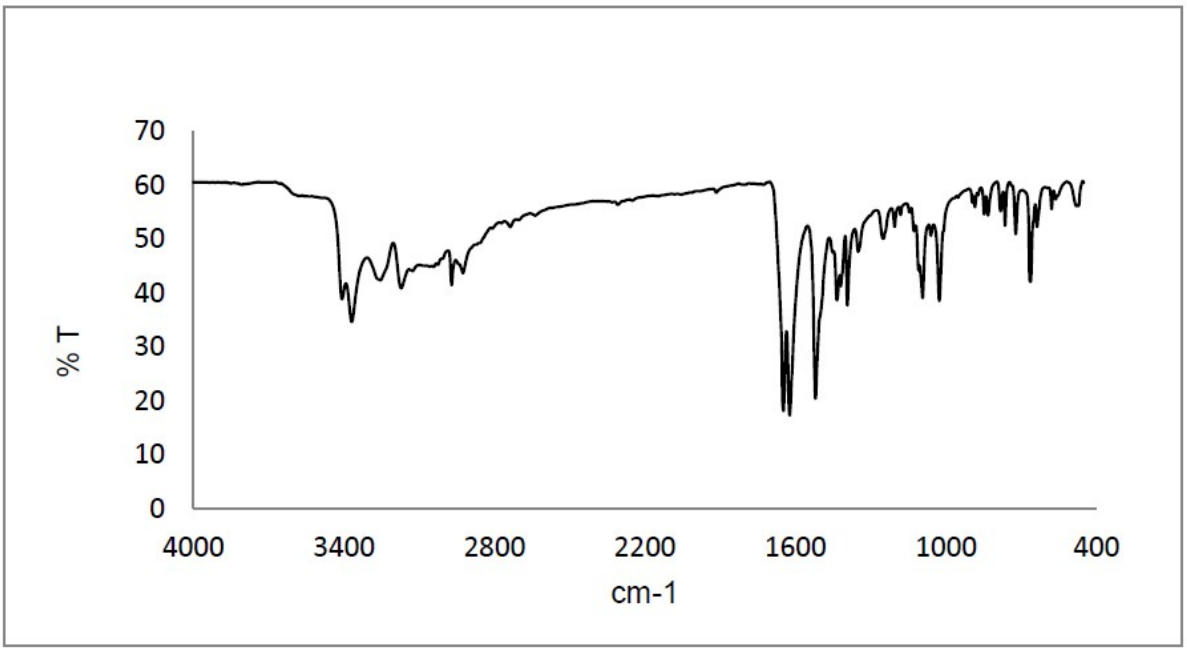

Fig. SF6 FT-IR spectrum of **1**·DMF.

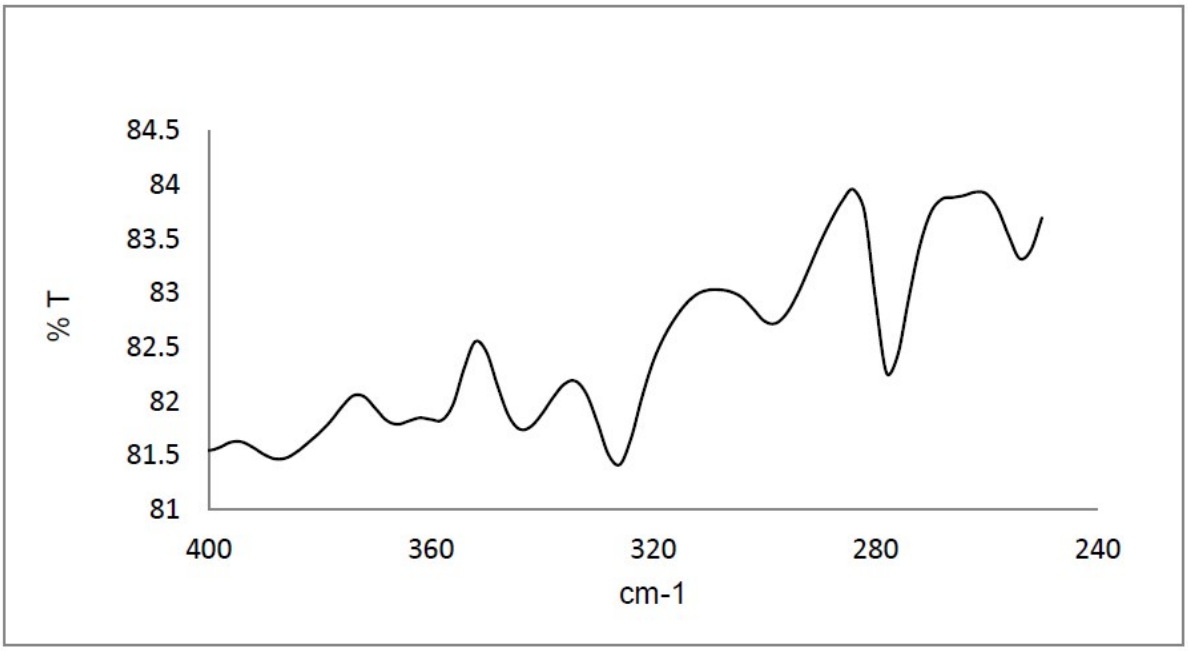

Fig. SF7 Far-IR spectrum of **1**·DMF.

Antibacterial activity

Table ST1 Colony numbers and the antibacterial rates for **L**-, **1**·DMF- and control samples against *E. coli* and *S. aureus* bacterial strains.

Microorganism	Sample	CFU/mL	Antibacterial rates (%)
E. coli **(*ATCC 25922*)**	**L**	1.0×10^4	99.33
	1·DMF	1.0×10^3	99.93
	Control	1.5×10^6	–
S. aureus **(*ATCC 6538*)**	**L**	2.4×10^5	84
	1·DMF	1.0×10^4	99.33
	control	1.5×10^6	–

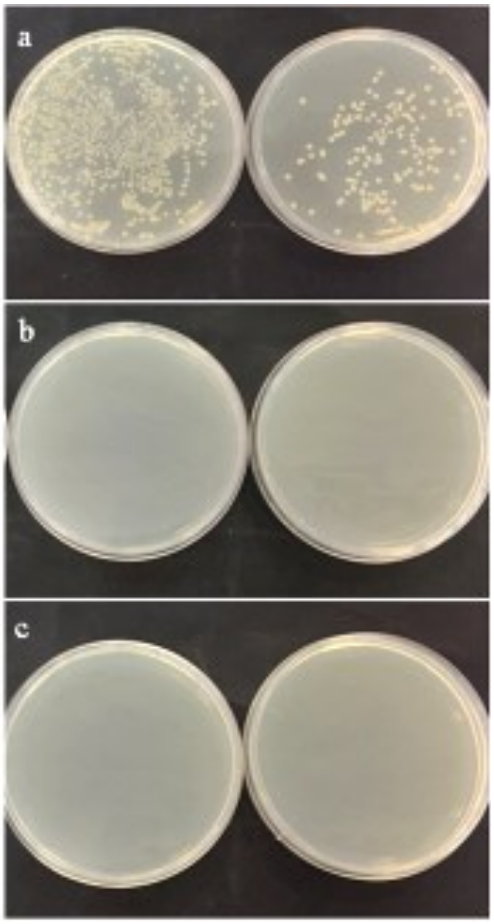

Fig. SF8 Typical photos of colonization by *E. coli* at 48 h of 10^{-3} (left), and 10^{-4} (right) dilution for (a) control sample, (b) **L** sample and (c) complex **1**·DMF sample.

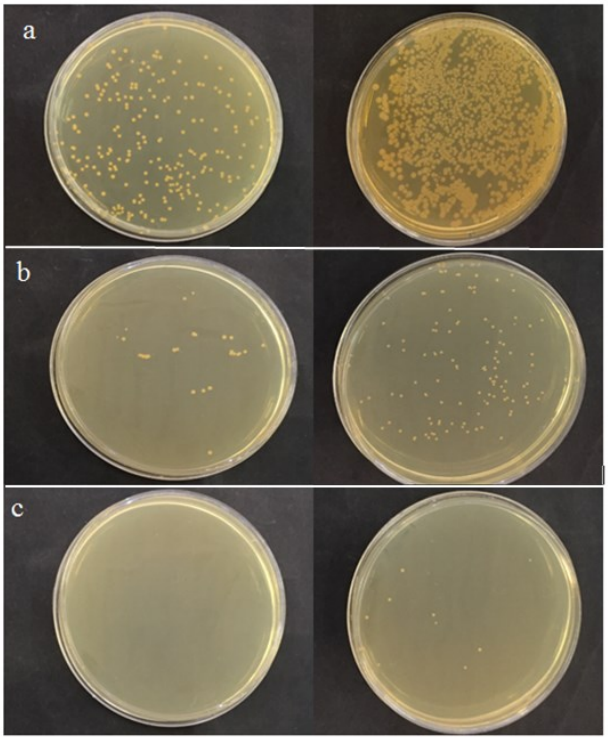

Fig. SF9 Typical photos of colonization by *S. aureus* at 48 h of 10^{-4} (left) and 10^{-3} (right) dilution for (a) control sample, (b) **L** sample and (c) complex **1**·DMF sample.

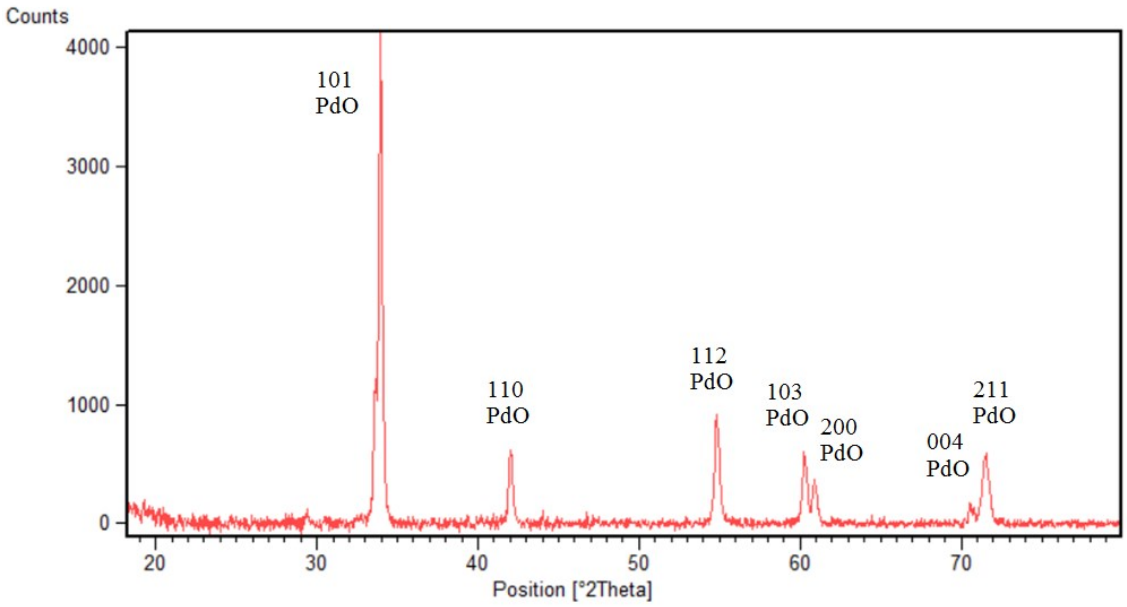

Fig. SF10 Powder XRD pattern of the product obtained from the solventless thermolysis of complex **1**·DMF at 600 °C in air.

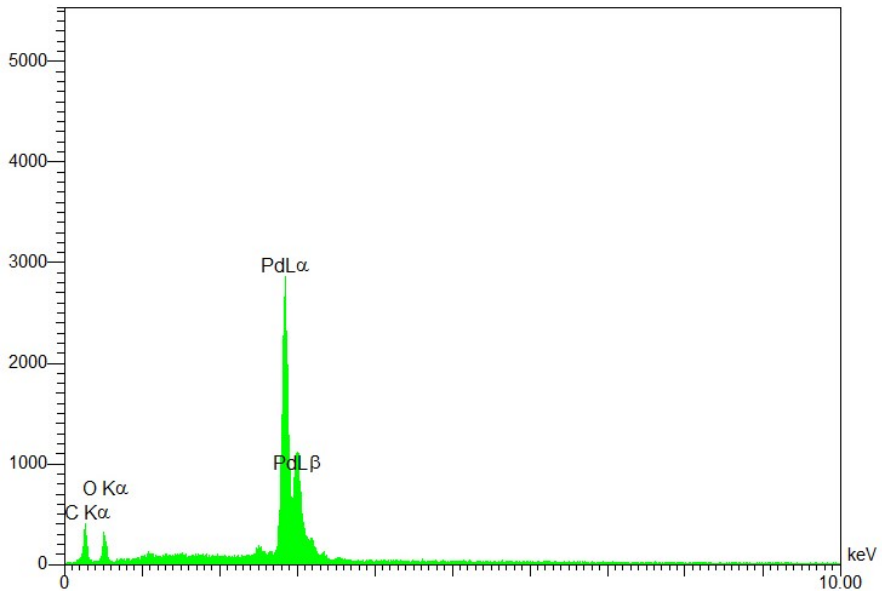

Fig. SF11 EDX analysis of the solventless thermolysis of complex **1**·DMF at 600 °C in air.

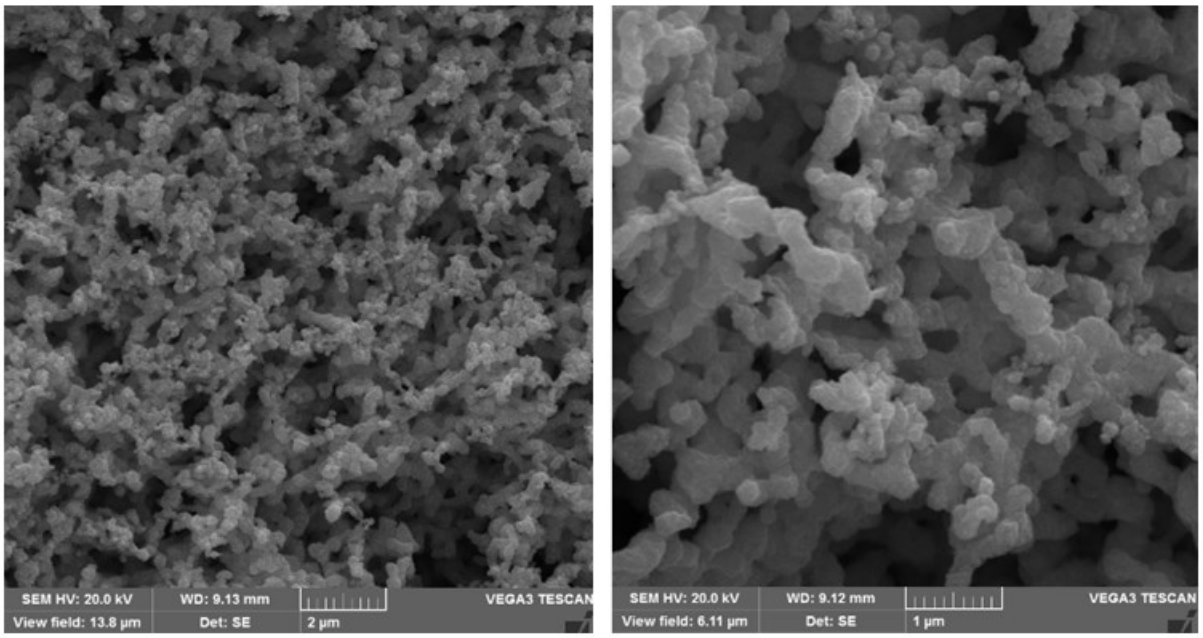

Fig. SF12 (a) Low-resolution SEM image and (b) high-resolution SEM image of PdO nanostructures formed by the solventless thermolysis of complex **1**·DMF at 600 °C in air.

References

1 N. S. Cho, J. G. Oh, H. J. Hwang, J.-G. Kim and Il-H. Suh, *Heterocycles*, 2002, **57**, 1919–1933.